XII International Conference on Computational Plasticity. Fundamentals and Applications
COMPLAS XII
E. Oñate, D.R.J. Owen, D. Peric and B. Suárez (Eds)

IMPROVEMENT OF IRREGULAR DTM FOR SPH MODELLING OF FLOW-LIKE LANDSLIDES

S. CUOMO*, M. PASTOR†, S. VITALE*, L. CASCINI*

* Labooratory of Geotechnics, Department of Civil Engineering
University of Salerno (UniSa)
Via Giovanni Paolo II, 84084, Fisciano (Salerno), Italy
e-mail: scuomo@unisa.it, s.vitale3985@gmail.com, l.cascini@unisa.it

† Department of Applied Mathematics, ETS de Ingenieros de Caminos,
Universidad Politecnica de Madrid (UPM),
Calle del Profesor Aranguren, 28040, Madrid, Spain
e-mail: manuel.pastor@upm.es

Key words: SPH, modelling topography, flow, landslide.

Abstract. Irregular topography of real slopes largely affects the propagation stage of flow-like landslides and accurate digital terrain models (DTMs) are absolutely necessary for realistic simulations and assessments. In this paper a simple yet effective method is proposed to improve the accuracy of existing DTMs which is applied to the topographical models used in well equipped laboratory experiments. Aimed at evaluating the effects of different DTMs in the results of the propagation modelling, a depth-integrated SPH model is used to simulate two series of laboratory tests referring to a frictional rheological model while using either the available DTM or the DTM improved through the proposed procedure. The obtained results show that the proposed method provides a more accurate topographical model for all the analyzed cases. Particularly, the new topographical model allows better reproducing the laboratory evidences in terms of run-out distances, inundated areas and geometrical characteristics of the final deposits. Furthermore, SPH analyses with progressively finer topographical inputs outline the role of DTM's precision towards the accuracy of the numerical simulations.

1. INTRODUCTION

Forecasting the susceptible propagation areas and the velocities of flow-like landslides is a crucial issue for risk analysis and the numerical modelling of the propagation stage is a valuable tool to predict these quantities in engineering analyses. However, the irregular topography of natural slopes considerably affects the motion of propagating material(s) and accurate Digital Terrain Models (DTMs) are fully necessary for realistic simulations and assessments.

Since last decades several numerical models have been developed to accurately simulate the time-space evolution of flow-like landslides as it concerns either the overall rheological behaviour or the possibility to capture the effects of local/micro peculiarities of the DTM such as narrow gullies, streets and channels. Among the available numerical approaches, the

Smoothed Particle Hydrodynamics (SPH) method fulfils the twofold requirement to: i) distinguish the accuracy of DTM from the spatial discretization of moving masses, ii) provide an efficient continuum-based discretization of the moving mass to reduce the computational times.

In this paper the “GeoFlow-SPH” model [1], [2] is used which discretizes the propagating mass through a set of moving “particles” or “nodes”. Particularly, the information, i.e. variables and their derivatives, is linked to the particles and the SPH discretization consists on a set of ordinary differential equations whose details are provided by Pastor et al. [1]. The accuracy of the numerical solution and the level of approximation for engineering purposes depend on how the nodes are spaced, as recently reviewed by Pastor and Crosta [3]. As input data, different DTMs are used to represent the topographical surfaces used in the laboratory experiments performed by Iverson et al. [4]. The potentialities of the proposed method for DTM improvement is tested comparing the results achieved for both the original DTM and the DTMs refined through the proposed procedure.

2. METHODS AND INPUT DATA

2.1. The proposed procedure for DTM refinement

In SPH modelling the topographical input can be represented by a list of point P_i (x_i,y_i,z_i) and/or a matrix including a finite element discretization of the domain.

Given a set of points P_i (x_i,y_i,z_i) with i=1…n, the proposed method provides: i) a new topographical model for the ground surface consisting in a new set of points P_j (x_j,y_j,z_j) with j=1…m and m>n; ii) a schematization of the topographical domain in a set of triangular elements; iii) a finer grid of squares for topography.

The first step is based on a Delaunay Triangulation (DT) [5] in the *xy* plane for a set of original points P_i (Fig. 1a); a new representation of the domain is obtained through a mesh of triangular elements (also called “Delaunay triangles”) which is usually referred as a Triangulated Irregular Network (TIN). Due to the properties of DT, it arises that: i) the resulting TIN is unique if the same algorithm is used; ii) the geometric shape of the resultant triangles is the optimum, i.e. each triangle is nearly equilateral if there are no specific conditions; iii) each triangle is formed with nearest neighbour points, i.e. the sum of the three edges of the triangle is minimum [5].

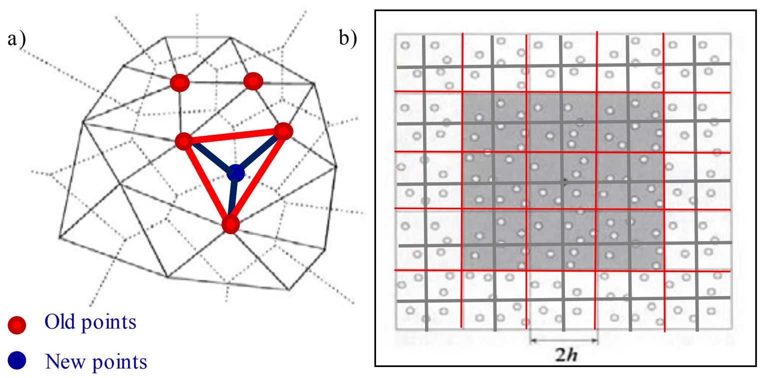

Figure 1: Schematic of the proposed procedure for DTM: a) points refinement, b) grid refinement.

The new points P_k (x_k,y_k), with k=1…l and l<m, are added to the topographical model; each point is located in the geometric barycentre of the Delaunay triangles, so a larger number of points is added in the areas where the topographical irregularity is much consistent. The height (z_k) of the new point is estimated by a scattered interpolation function (TriScatteredInterp by MatLab). The final topographical model P_j will be composed by the P_i points of the original model in addition to the new P_k points (approximately m≈2.6n). As second step of the procedure, a Delaunay Triangulation is performed among the P_j points to a finite element mesh for domain discretization. As final step, a finer grid of squares (usually referred as GRID) is obtained for topography and is used for SPH computation (Fig. 1b).

In this paper, the procedure is tested for well equipped laboratory experiments performed by Iverson et al. [4].

2.2 Experimental evidence from flume tests

Iverson et al. [4] and Denlinger and Iverson [7] investigate the propagation of a dry sand mass over an irregular basal topography in two series of experiments using a flume 0.2 m wide and about 1 m long (Fig. 2). Particularly, an irregular urethane basal surface is used with two distinct topographic configurations: i) in the experiment A, namely "regular" configuration, the urethane support reproduces two gullies joining at the toe of the slope, ii) in the experiment B, namely "inverted" configuration, the urethane support was rotated by 180° and the propagating mass travels first in a main gully and then in two minor channels. In both cases, the head of the flume is fitted with a vertical glass head gate for release a static granular mass, thus initiating the flow [4].

In both experiments, quartz sand is used with angular grains of 0.5 ÷ 1 mm diameter in the experiment A while rounded grains of 0.25 ÷ 0.5 mm diameter in the experiment B. The sand properties for the experiments A and B are resumed in Table 2.

The experimental evidences are acquired through both a series of snapshots of the propagating mass and a laser cartographic technique. The achieved data show a considerable variation of the width and the cross section of the flow in both time and space, i.e. it is well reproduced the full 3D features of the sand motion usually observed in real cases. Despite the difference in the topographic configuration of the flume bed and despite the variations in the sand properties, in both the experiments A and B similar maximum speeds and run out distances are recorded, respectively, equal to about 1 m/s and 0.52 m. Particularly, figure 3 represents the isopach maps of vertical flow height "h" and further information about this study can be found in Iverson et al. [4].

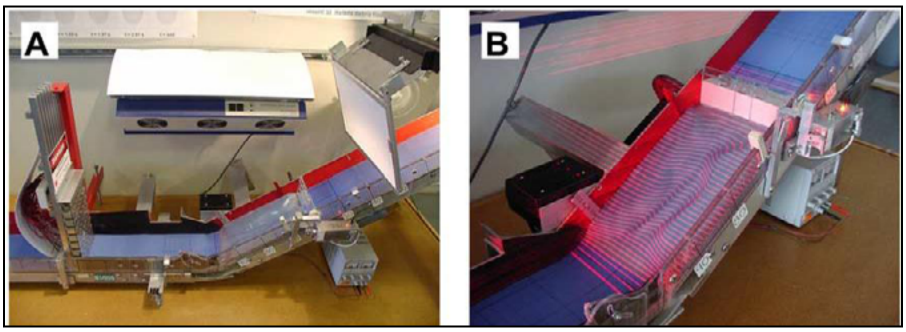

Figure 2: Lateral (a) and oblique (b) photos of the flume used in the flow experiments [4].

Table 1: Properties of sands used in the experiments of Iverson et al. [4].

Properties	A	B
Diameter of sand grains (mm)	0.5 ÷ 1	0.25 ÷ 0.5
Sand volume (cm^3)	308	308
Sand bulk density (g/cm^3)	1.26	1.55
Basal friction angle sand on urethane (°)	19.85	22.45
Internal friction angle of sand (°)	43.99	39.39

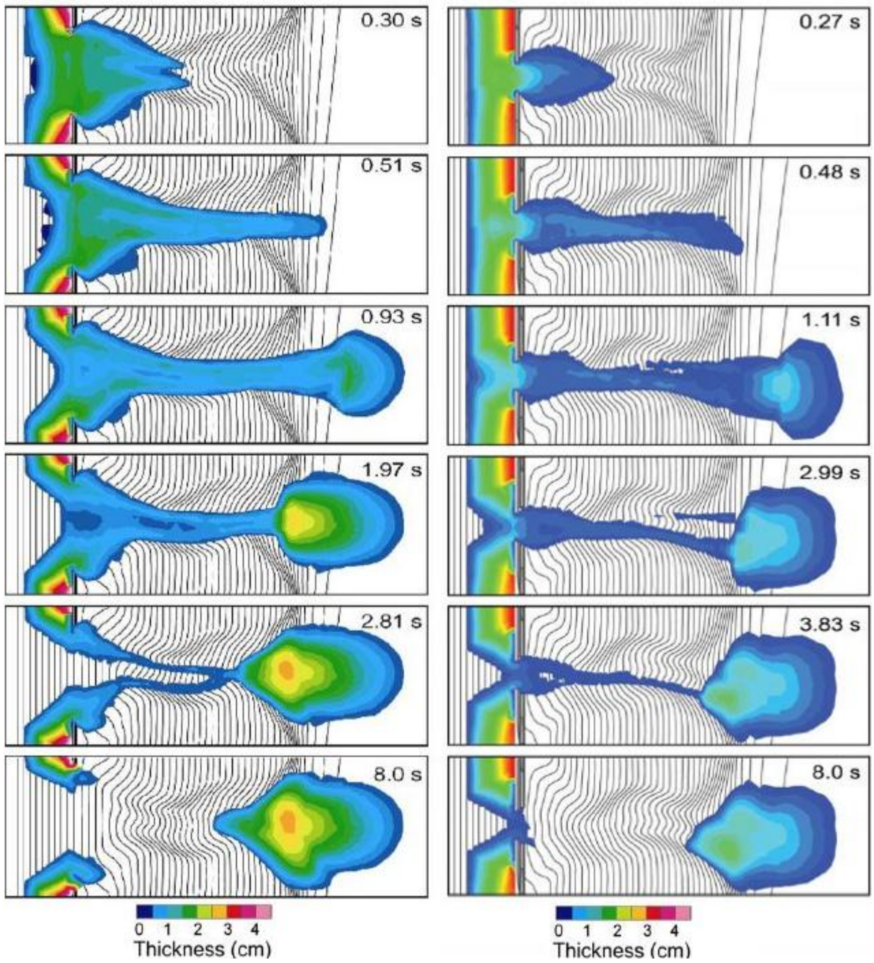

Figure 3: Isopach maps of flow vertical thickness in the experiment A (on the left) and B (on the right) [4].

3. APPLICATIONS OF DTM REFINMENT PROCEDURE

The results of the proposed procedure are provided in figure 4 which outlines the achievable refinement of the topography used in the experiment A of Iverson et al. [4].

In this case the original DTM consists of 1895 points (1.9 points/cm^2) representative of the 55 elevation contour lines "z"; on the other hand, the refined DTM "A1" has 5186 points and 111 contour lines with a density of 5.2 points /cm^2 (Table 1). As far as Delaunay triangles, they increase from 3771 to 9805 and their dimension reduces from 0.54 ÷ 5.4 cm to 0.28 ÷ 2.51 cm; it entails that the background grid for SPH computation consists in squares whose dimension is reduced from 1.2x1.2 cm to 0.6x0.6 cm. A multiple-application of the proposed procedure allows a progressive improvement of the original DTM, as reported in table 3. Analogously, for experiment B, one application of the refinement procedure provides an increase of points from 1788 to 4837 and triangles from 3519 to 9545 whose dimensions reduce from 0.65-5.40 cm to 0.28-2.20 cm (DTM B1). Thus, the squares for SPH computation reduce from 1.2x1.2 cm to 0.6x0.6 cm.

As far as the dimension of DTM squares reduces, the number of SPH particles is increased thus providing a higher accuracy of the final results (Tab. 3). It is worth noting that the accuracy for the description of interactions among SPH particles is kept unchanged by not reducing the dimension of the kernel function (to this aim the product of DTM square dimension times the factor "Fact-hsml" is kept constant, details are given in Pastor et al. [1]).

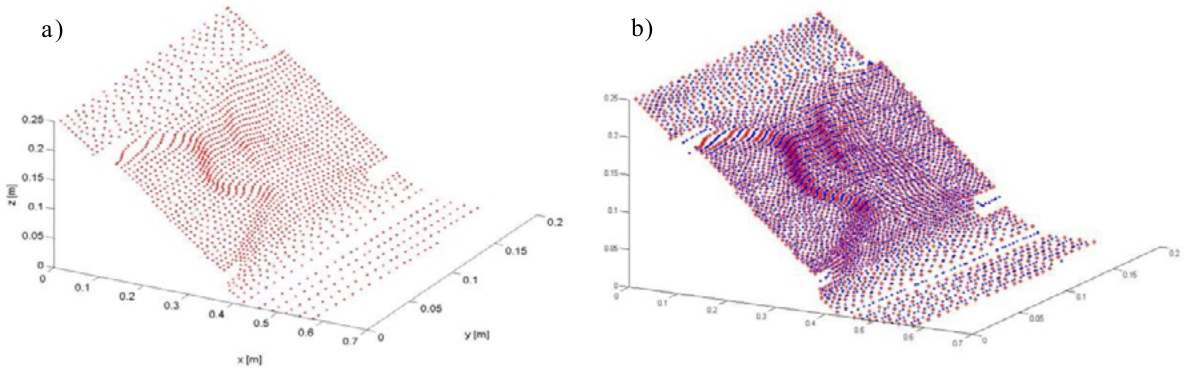

Figure 4: a) Original and b) refined DTM for the experiment A of Iverson et al. [4].

Table 3: Properties of the original and refined DTMs for experiment A and B.

Properties	Experiment A				Experiment B			
	Original	A1	A2	A3	Original	B1	B2	B3
Number of DTM points	1895	5186	15203	44522	1788	4837	14009	40977
Density of DTM points (points/cm^2)	1.9	5.2	15.2	44.6	1.8	4.9	14.0	41.1
DTM squares grid (cm)	1.2	0.6	0.4	0.2	1.2	0.6	0.4	0.2
SPH Particles	518	1040	1536	3094	518	1040	1536	3094
Fact-hsml	2	4	6	12	2	4	6	12

4. NUMERICAL SPH ANALYSIS

4.1. Experiment A

SPH simulations are carried out for different DTMs, the "original" and "refined" DTMs named A1, A2 and A3. The GeoFlow-SPH model [1] is used referring to a frictional rheological model which takes also into account the effect of slope curvature on the propagation of the mass (details are provided by Pastor et al. [1]). In both cases, soil mechanical properties are taken from table 2 and the initial soil mass consists in a 0.2 m wide source area with boundary conditions fixed in agreement with Iverson et al. [4].

The propagation heights of the soil computed at different time steps are shown in figure 5 for point P. Firstly, propagation occurs at point “P” (Fig. 5) and then a second surge of material causes propagation and deposition. On the other hand, the velocities are slightly overestimated in both cases with a better evaluation for the improved DTMs. Particularly, all the simulations satisfactorily reproduce the global behaviour of the sand over the slope (Fig. 6) as well as the height of the flow during the propagation stage. The simulated shape of the final deposit is slightly different for the “original” and the “refined” DTMs (cases A1, A2 and A3). In the former case, the simulated mass deposit is symmetrical in both the x and y directions differently from the experimental evidence. In the latter cases, a twofold lobe morphology is reproduced for deposit, with a distal lobe and proximal talus slope, in agreement with the experimental data. Furthermore, the distal deposit is formed during the initial surge, while the talus slope is accreted when a surge of material arrives at the deposition area.

Finally, figure 7 outlines the spatial-temporal propagation pattern for the case A1 which is allows simulating the experimental evidences (Fig. 3a) with a moderate computational effort.

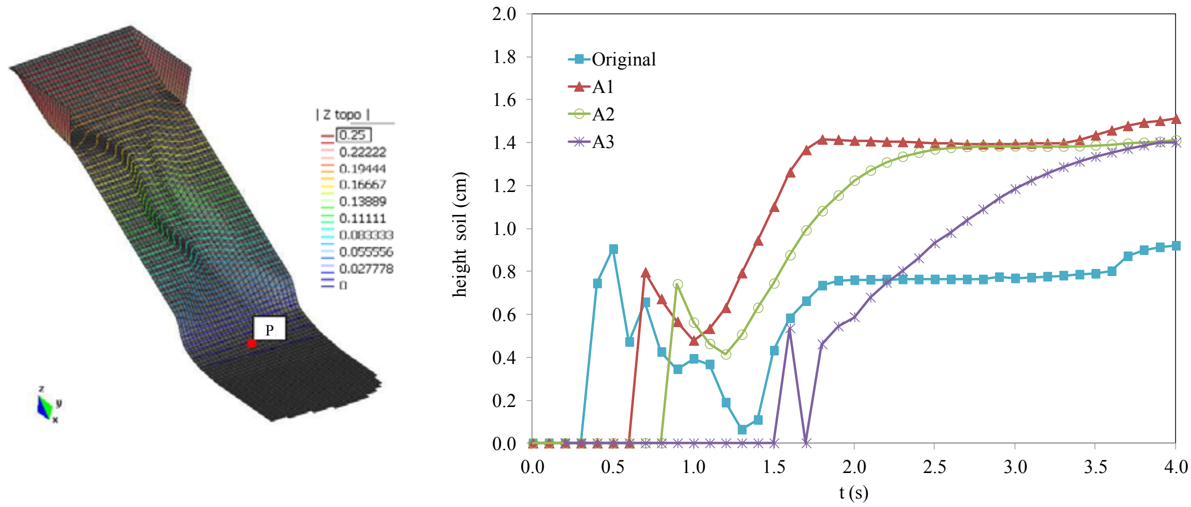

Figure 5: Simulated height of soil for Point “P” for the “original” and “refined” (A1, A2 and A3) DTMs.

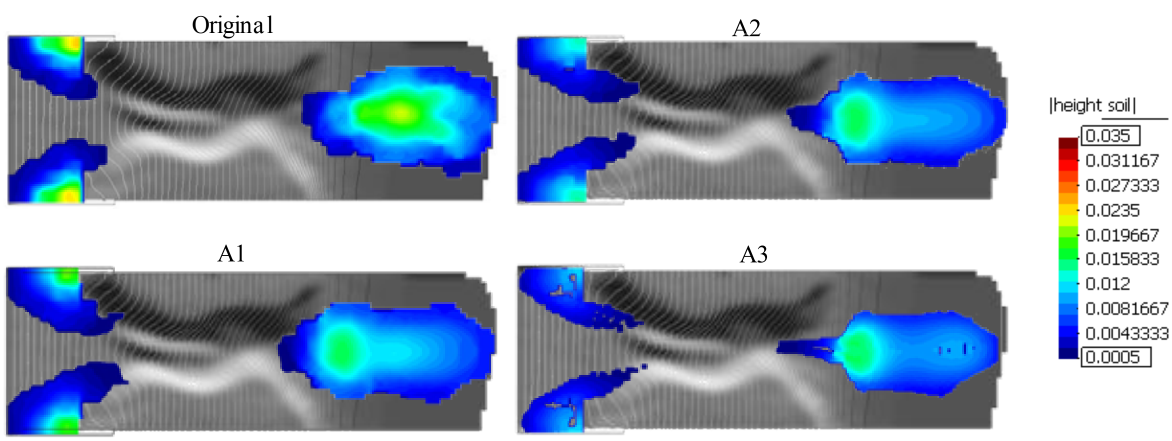

Figure 6: Final soil deposit simulated for the “original” and “refined” (A1, A2 and A3) DTMs.

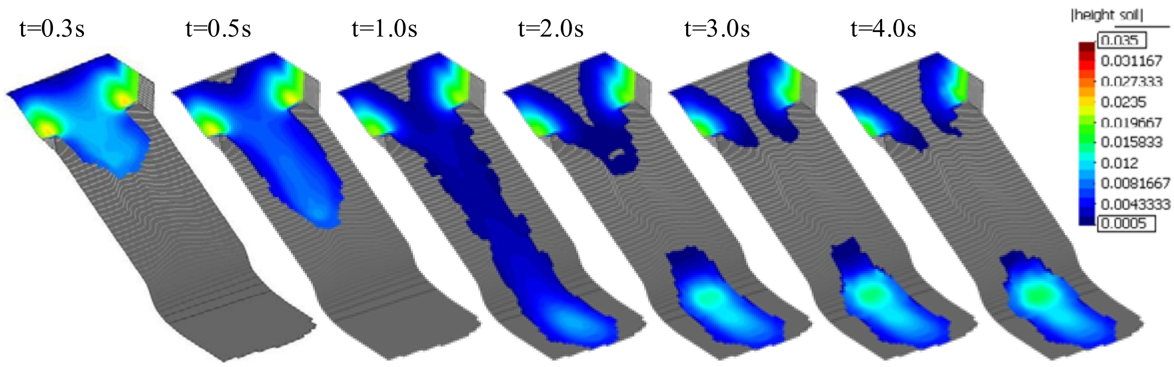

Figure 7: Simulated height of soil for the "refined" DTM A1.

4.2. Experiment B

Aimed at testing the DTM refinement procedure for another well documented case, SPH simulations are carried out also for the experiment "B". Particularly, all of the simulations share the same input data in terms of mechanical characteristics of the material (Table 2), selected rheological model (pure frictional fluid with influence of the curvature of the topography) and boundary condition while referring to different DTMs: the original "original" DTM and the "refined" DTMs named B1, B2 and B3. Figure 8 shows the simulated heights of soil at different time steps for the above mentioned cases. In agreement with the previous case study, the "GeoFlow-SPH" model provides a satisfactory match with the experimental results. The global behaviour of sand propagation and the heights of soil are well predicted. Figure 8 shows that the numerical simulations estimate a higher height of soil for the point "Q" situated upstream, especially in the first part of the motion; this indicates that in the real experiment, the movement of the sand is more gradual and the deposit is less thick but longer, while in all of the simulations for refined DTMs the motion is more "impulsive" and the deposit is thicker and shorter.

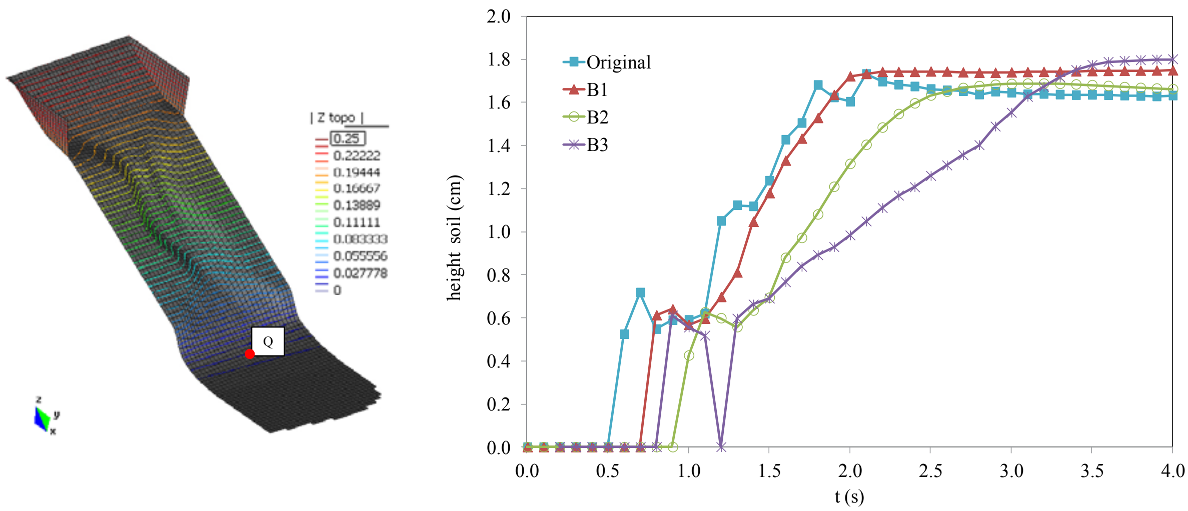

Figure 8: Simulated height of soil for Point "Q" for the "original" and "refined" (B1, B2 and B3) DTMs.

Furthermore, while in the experiment A the deposit was situated at the centre of the flume bed and the lateral secondary deposits are quite symmetrical to the axis, in this case the deposit is slightly asymmetric at the left-hand side of the channel. This evidence cannot be captured with the "original" DTM while an improvement is achieved with refined DTMs even though the results don't match perfectly the real experiment, as shown for point "Q" located downstream. As also the Authors of the experiments point out [4], the differences between the observed and computed geometry of soil deposits largely result from dispersion of the distal margin due to sand saltation, especially for the spherical sand (experiment B). This discrepancy is logic considering that the mathematical model here used does not represent the physics of particles saltation.

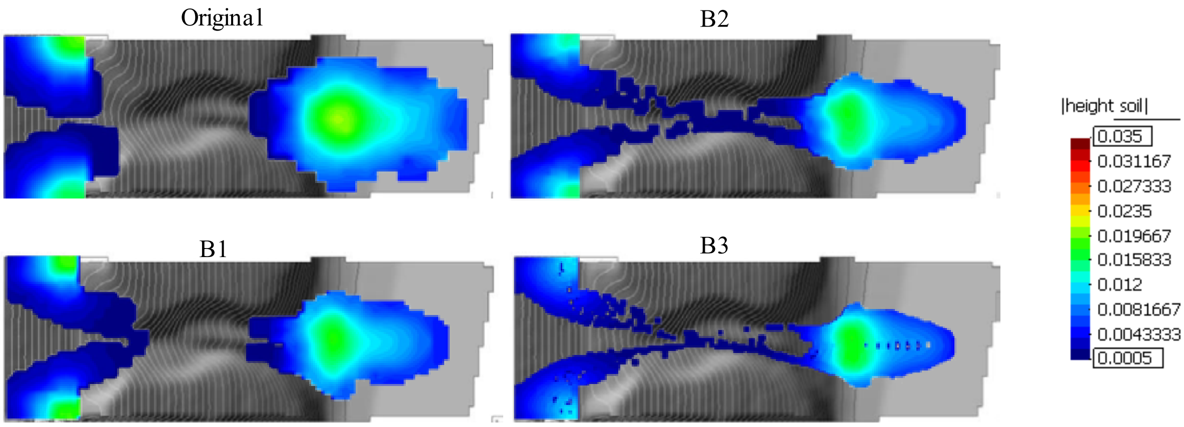

Figure 9: Final soil deposit simulated for the "original" and "refined" (B1, B2 and B3) DTMs.

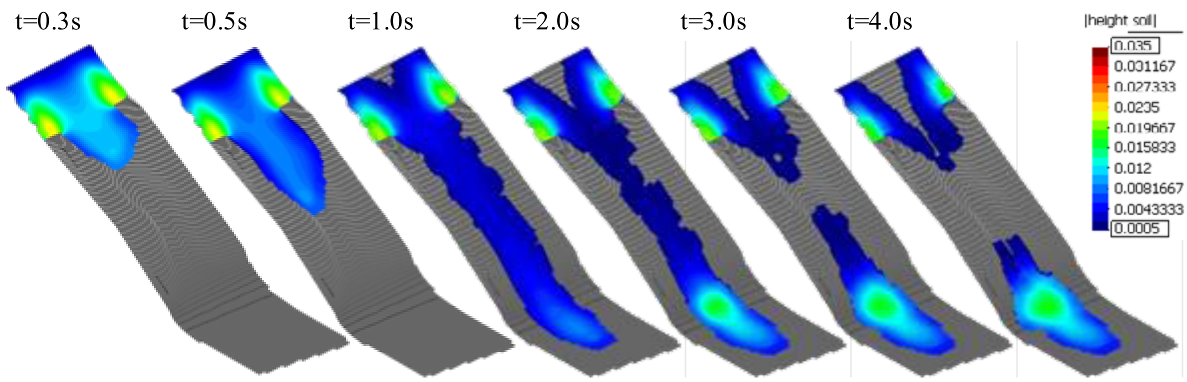

Figure 10: Simulated height of soil for the "refined" DTM B1.

4.3. Discussion

The comparison of the achieved results allows providing some considerations about the potentialities of the proposed procedure and the reliability of the obtained results. Firstly, the application of a 1-step DTM refinement (cases A1 and B1) significantly improves the quality of the results with moderate efforts as far as the computational times and the memory storage of information. On the contrary, a multiple application of the DTM refinement procedure is useless as it increases the computational time and memory requirements while not improving significantly the results as it concerns the simulated global behaviour and specific local effects.

Table 4: Properties of the original and refined DTMs for experiment A and B.

Properties	Experiment A				Experiment B			
	Original	A1	A2	A3	Original	B1	B2	B3
Number of DTM points	1895	5186	15203	44522	1788	4837	14009	40977
DTM squares grid (cm)	1.2	0.6	0.4	0.2	1.2	0.6	0.4	0.2
SPH Particles	518	1040	1536	3094	518	1040	1536	3094
Facthsml	2	4	6	12	2	4	6	12
Time discretization (s)	0.001				0.001			
PC computational time (min)	6	31	82	494	6	31	90	515
File Dimension (Mb)	7.37	22.68	44.83	158.13	7.22	22.33	44.03	153.83

4. CONCLUSIONS

The analysis and forecasting of susceptible propagation areas and velocities of flow-like landslides are crucial issues for risk analysis. To this aim, numerical modelling of the propagation stage is a valuable tool and many efforts have been devoted to obtain accurate digital terrain models (DTMs) which are absolutely needed for realistic.

In this paper a simple yet effective method is proposed to improve the accuracy of existing DTMs which is applied to the topographical models used in well equipped laboratory experiments. The procedure allows adding new elevation points to a given set of points, also providing a schematization of the topographical domain in a set of triangular elements and a grid of squares whose dimensions are smaller than the initial ones. A depth-integrated SPH model is used to simulate the propagation stage of the selected experiments and the effects of different DTMs are evaluated towards the achievable results from propagation modelling. To this aim, a frictional rheological model is used while referring to either the available DTM or the DTM refined through the proposed procedure. The obtained results show that the proposed method provides a more accurate topographical model for all the analyzed cases. Particularly, the new topographical model allows better reproducing the laboratory evidences in terms of run-out distances, inundated areas and geometrical characteristics of the final deposits. On the other hand, it is shown that a multiple application of the refinement procedure increases the computational time and memory requirements while not improving significantly the results as it concerns the simulated global behaviour and specific local effects.

REFERENCES

[1] Pastor M., Haddad B., Sorbino G., Cuomo S. and Drempetic V. *A depth-integrated, coupled SPH model for flow-like landslides and related phenomena*. Int. J. Numer. Anal. Meth. Geomech. (2009) **33**:143-172.

[2] Cascini, L., Cuomo, S. and Pastor, M. *Geomechanical modelling of debris avalanches inception.*

Landslides, (2012), DOI 10.1007/s10346-012-0366-0.

[3] Pastor, M., Crosta, G.B. *Landslide runout: Review of analytical/empirical models for subaerial slides, submarine slides and snow avalanche. Numerical modelling. Software tools, material models, validation and benchmarking for selected case studies*. Deliverable D1.7 for SafeLand Project, http://www.safeland-fp7.eu/results/Documents/D1.7_revised.pdf (2012), 1-44.

[4] Iverson, R.M., Logan M. and Denlinger R.P. *Granular avalanches across irregular three-dimensional terrain: 2. Experimental tests*. Journal of Geophysics Research, (2004) **109**: 1-16.

[5] Delaunay B. *Sur la sphère vide*. Izvestia Akademii Nauk SSSR, Otdelenie Matematicheskikh i Estestvennykh Nauk, (1934) **7**: 793-800.

[6] Liu M.B. and Liu G.R.. *Smoothed Particle Hydrodynamics (SPH): an Overview and Recent Developments*. Arch Comput Methods Eng (2010) **17**: 25-76.

[7] Denlinger R.P and Iverson R.M.. *Granular avalanches across irregular three-dimensional terrain: 1. Theory and computation.* Journal of Geophysics Research, (2004) 109, 1-14.